New evidence of late Holocene relative sea-level stability on the Banc d'Arguin (Mauritania)

Raphaël Certain, Dia A Abdoul, Nicolas Aleman, Nicolas Robin, Robert Vernet, Jean-Paul Barusseau, Olivier Raynal

New evidence of late Holocene relative sea-level stability on the Banc d'Arguin (Mauritania)

Raphaël Certain [(a)], Abdoul Dia A. [(b)], Nicolas Aleman [(a)], Nicolas Robin [(a)], Robert Vernet [(c)], Jean-Paul Barusseau [(a,*)] and Olivier Raynal [(a)].

[a] *Centre de Formation et de Recherche sur les Environnements Méditerranéens, UMR-5110, University of Perpignan Via Domitia - CNRS, 52 avenue Paul Alduy, 66860 Perpignan Cedex 9, France*

[b] *Institut Mauritanien de Recherche Océanographique et des Pêches, BP22 Nouadhibou, Mauritania.*

[c] *Institut Mauritanien de Recherche Scientifique, BP 5055 Nouakchott, Mauritania.*

* Corresponding author.

Email adress: brs@univ-perp.fr (J.-P. Barusseau)

Keywords: Banc d'Arguin; Sea level curve; Shell middens; Prograding sand flats; Ice melting; Sedimentary units; Elevation measurements

Abstract

Morphological investigations on the northwest coastal plain of Mauritania (Banc d'Arguin) lead to a revised late Holocene sea-level curve. The region is characterized by extensive sand flats occasionally surmounted by low sand barriers. These barriers pick out a set of paleoshorelines attributed to the six episodes defined by Dia (2013). Morphological

evidence of the extreme flatness of the coastal plain is provided by topographic transects based on total-station surveys. Index points distributed throughout the late Holocene are defined in relation to the position of the barrier sole, which is adjusted to the upper limit of the berm uprush. The elevation of index points is related to the mean sea level (MSL) through an assessment of the various errors likely to affect the results. Over the period since ca. 7000 cal yr BP, the measured elevations remain within a few decimetres of the present-day sea level. This implies that, throughout this time interval, sea level in the Mauritanian region oscillated within the usual range of natural variations, whereas oscillations of larger magnitude prevailed elsewhere. Because the study area is tectonically stable, the glacio-eustatic adjustment due to hydro-isostatic effects is of minor importance in Mauritania and the relative sea level (RSL) has responded solely to the eustatic component. Therefore, we would expect to find some record of ocean syphoning through a gradual emergence of the land after the mid-Holocene marine transgression and the subsequent development of vertically stepped paleoshorelines. The absence of such evidence raises the question of whether the drop in RSL was compensated by continuing deglaciation during the late Holocene.

1. Introduction

Current changes in sea level need to be regarded in the light of the complexity of earlier sea level changes, which allow us to extend our knowledge of their mechanisms and variability on a longer time scale. An improved knowledge of post-glacial variations in relative sea level (RSL) over the last six millennia (late Holocene) would lead to a better understanding of the current functioning of the Earth system (Pirazzoli, 1991). During the late Holocene, sea level in low and mid latitudes has only fluctuated by approximately 1-3 m

around its current elevation (e.g. Woodroffe and Morton, 2005; Sloss et al, 2007, for the Indo-Pacific).

Many recent studies (Barlow and Shennan, 2008; Wanner et al., 2008; Shennan et al., 2009; Engelhart et al., 2011; Tamisiea and Mitrovica, 2011), have shown that these changes in RSL generally display a spatial and temporal variability. Among the forcing mechanisms influencing RSL during the late Holocene, the varying rate of ice melting (i.e. the glacio-eustatic signal) plays a dominant role in causing these variations. Many studies have attempted to establish the characteristics of this signal, by taking into account all possible disturbing mechanisms: isostatic consequences of changes in ice mass distribution, steric effects, latitudinal zonation and regional factors (Woodroffe and Horton, 2005).

Geophysical modelling can be used to identify and validate several types of RSL variation reflecting the real effects of deglaciation due to progressive melting of the ice sheets between 18,000 and 5,000 years BP, which is the estimated date of the end of glacial retreat (Fig. 1). Depending on the sector considered, RSL variation curves reflect episodes of submergence, emergence or stability throughout the late Holocene (Clark et al., 1978; Peltier, 2002; Shennan and Horton, 2002; Lambeck et al., 2003; Mitrovica, 2003). In fact, it is easier to establish the contribution of eustatic variations based on local sea-level history in far-field locations remote from glaciated areas at higher latitudes, thus reducing the effects of disturbing mechanisms (Peltier, 2002). At low latitudes, the local history of RSL variation is represented in curves of type III (after a slight rise above the current sea-level value, RSL then falls back to its present-day position), IV (strong attenuation in the rate of RSL rise over the last five millennia), V (emergence of 1 to 3 m at around 5,000 BP, as illustrated by many

mid-Holocene highstands) and VI (effects observed in other zones combined with effects related to flexure of the continental margins and shelves).

Despite numerous studies, variations of sea level during the late Holocene still appear very complex and new data are required to improve our understanding of these fluctuations, especially in regions that have been little studied. Such is the case in West Africa, particularly in Mauritania, a region which is difficult to access for practical and geopolitical reasons and which therefore suffers from a lack of in-depth studies. In this paper, we address the problem of late Holocene sea-level variability in north-western Mauritania based on the investigation of sedimentary units on the coastal plain. The Gulf of Arguin, situated between latitudes 19°20'N and 21°10'N), corresponds to a far-field location remote from glaciated areas, which provides the opportunity of establishing a new RSL curve for this part of West Africa.

2. Study area

2.1 Geological framework

The north-west coast of Mauritania is bordered by the Gulf of Arguin (Fig. 1), a part of the Senegalo-Mauritanian sedimentary basin, bounded to the north-east by an ancient uplift block forming the stable cratonic chain of the Mauritanides (Potrel, 1994). Overall, this region is characterized by a highly stable tectonic regime. Ancient major tectonic events are dated as Archean in the Reguibat shield (Potrel et al., 1998) and Neo-Proterozoic to Cambrian in the Mauritanides chain (Hamoud et al., 2015). From a geophysical point of view, the continental shelf is located near the boundary between zones III and IV of Clark et al. (1978). The terrestrial part of the coastal basin consists of Mesozoic, Cenozoic and

Quaternary formations. The older formations are poorly exposed, primarily at the periphery of the basin, and are generally only encountered in boreholes. The Quaternary, on the other hand, is largely represented by surface deposits, which are classically described as a sequence of marine deposits separated by continental facies corresponding to phases of sea-level fall (Faure and Elouard, 1967; Hébrard, 1973; Einsele et al., 1977). The post-glacial sedimentary record in North-West Africa is characterized by marked climatic variations (Lancaster et al., 2002), especially during the Holocene (Lezine et al., 2011). In a domain largely open to the Atlantic Ocean, these climate changes could have impacted the final stages of the postglacial transgression during the late Holocene. In the Banc d'Arguin (BA) area, early studies proposed that the sea-level reached a highstand of about +2 to 3 m before falling to its present position (Hébrard, 1973; Elouard, 1975; Faure et al., 1980). The transition between the highest sea-level stand and the present-day level would have occurred in several stages during which the sea level oscillated between +3 and -3.5 m (Einsele et al., 1974; 1977). This pattern is similar to RSL curves described from other regions (Angulo et al., 2006; Sloss et al, 2007; González and Törnqvist, 2009; Castro et al, 2014). However, more recent studies have called into question this model, which is not in conformity with the facts (Barusseau et al., 2007).

2.2 Geomorphology of the coastal plain

The coastal plain of the Gulf of Arguin extends along the border between the Atlantic Ocean and the Sahara, from Cap Blanc to Cap Timiris (Fig. 1). It extends over more than 200 km with a width varying from 0 to 12 km and forms the prolongation of the shallow internal basin of the Gulf of Arguin (with maximum water depths of 20 m), which is separated from the open sea by a shallow rocky sill (less than 2-5 m deep), the Banc d'Arguin itself (Aleman et al., 2014). The coastal plain consists of several kilometres of wide sand flats and linear

sandy ridges, the latter being generally a few dm in height, but exceptionally more than 1 m (Barusseau et al., 2007, 2009, 2010). The sand flats and ridges are composed of fine sands and rare gravels (D50 between 0.15 and 0.25 mm), with homogeneous facies and without apparent internal structure (Fig. 2A). Most of the sandy linear ridges are covered by dm-thick Neolithic shell middens (Barusseau et al., 2007) containing *Senilia (=Anadara) senilis* (Lavaud et al., 2013) and varying in age from 6730 to 2520 cal yr BP (Vernet, 2014). The sandy ridges separated by large sand-flat surfaces form a series of low barriers between the land and the present edge of the coastal plain. They correspond to different beach structures formed by the joint action of low-energy waves and wind, according to a model described by FitzGerald and Buynevich (2005). Sometimes, these structures correspond to sedimentary spits, primary dunes (Sloss et al., 2012), or simply beach berms. In the following, these co-genetic landforms are referred to as "barriers". These various kinds of barrier represent successive positions of paleo-shores during the development of the late Holocene coastal plain (Dia, 2013).

On the inland side, the limit of the plain is often marked by the presence of cliffs of variable elevation, cut in Pleistocene rocky formations (Fig. 2A). The presence of numerous tide marks shows that these vast stretches of slightly tilted (gradients less than 1/1000 to 1/10000) tidal sand flats can be episodically invaded by the sea up to several kilometres inland from the shoreline (Fig. 2B). In some instances, modern linear dune ridges and barchan dunes cover the late Holocene morphological units without any genetic connection with the Holocene coastal plain units.

2.3 Sediment supply to the coast

According to climate data, the region can be classified as a cool tropical coastal desert. The Gulf of Arguin is swept by powerful offshore winds (NE Trades) transporting vast quantities

of aeolian dust from the Sahara to the west and providing massive amounts of fine sand and silts to the coastal areas. All segments of the BA coastal plain can be considered as being influenced by these winds and the resulting sand transport, as shown by the extension of old ergs and the current dune massifs (Lancaster et al., 2002). Depositional processes are of major importance in the absence of permanent drainage network due to the current lack of fluvial inputs in the study area. However, exceptional heavy rains can reactivate sediment transport in paleo-wadis, which are remnants of an extensive but currently inactive ancient fluvial system (Vörösmarty et al., 2000; Skonieczny et al., 2015). These wadis may have been active at different times in the late Holocene, but are currently not associated with any significant sediment transport (Dia, 2013).

2.4 Hydrodynamic forcing

The mean tidal range in the study area varies between 1 m (neap tides) and a maximum of 2 m (spring tides). The swell comes mainly from the north-west sector for nearly 50% of the time; from June to August, south-westerly waves are associated with the monsoon. According to Topex-Poseidon data, the significant wave height of the swell off Mauritania varies from 2.7 m in December-January to 1.7 m in May-June (Thomas and Senhoury, 2007). However, due to the sheltering effect of the Banc d'Arguin rocky shoals and the shallowness of the inner platform, the waves have a limited effect on the shoreline which can be considered to be subject to a low-energy regime (Dia, 2013). During the monsoon period, surges can occur causing flooding of the coastal plain. A quasi-permanent N-NW wave climate prevails in the Arguin basin generating a longshore drift from north to south, ensuring distribution of sediments, forming many rapidly evolving sand spits. During the late Holocene building up of the coastal plain, the action of marine processes led to a spreading out of the abundant input of aeolian sand over the intertidal zone (Fig. 2C and D), forming

sand-flats and episodically, on the sand-flats, a series of sand barriers, rapidly covered by anthropic shell middens.

To summarize, the BA coastal plain is made up of a vast flat expanse characterized by the juxtaposition of sedimentary units of two kinds, sand flats and barriers, which were formed during a continuous late Holocene progradation resulting from considerable aeolian sedimentary supply reworked by coastal marine processes. In such a context, the sea-level changes assumed by Einsele et al., (1974, 1977) would have resulted in late Holocene highstand deposits during periods of rising sea level and incision marks during phases of regression and subaerial weathering. However, in more recent studies, late Holocene coastal deposits have been found at elevations that are within the range of modern wave and tidal action (Barusseau et al., 2007, 2009 and 2010; Dia, 2013), thus casting doubt on late Holocene sea-level fluctuations (Aleman et al., 2014). The results presented below provide several comprehensive lines of evidence that may resolve this apparent paradox in a satisfactory way.

3. **Methods**

One difficulty in studying sea-level variations in the late Holocene is the quality of measurements used to establish the RSL curve (Edwards, 2005; Kelletat, 2005; Sloss et al., 2007; González and Törnqvist, 2009). These data have often been criticized for the insufficient number of ages and lack of precision of topographic or bathymetric data, causing misinterpretations (Angulo et al., 2006; Baeteman et al., 2011). During seven field campaigns between 2005 and 2010, detailed attention was therefore paid to reducing these margins of uncertainty. The essential objective of this fieldwork was to specify the geometry of the

coastal plain and its associated barriers (apart from the present-day barchan ridges) in relation to the coeval sea-level variations.

3.1 Identification of paleo-shorelines

The reconstruction of late Holocene paleo-shorelines is facilitated by the favourable combination of two factors. First, Neolithic populations were attracted on several occasions to areas above the high tide mark where sandy features of low relief were developed on the sub-horizontal substrate of the sand-flats (Fig. 2C and D). These groups stockpiled shells of *S. senilis* harvested on the neighbouring foreshore (Vernet, 2007), as observed in many parts of West Africa (Descamps et al., 1974). The second factor is the armouring of sandy landforms produced by the white covering of shells (Fig. 2C and A). As a result, the preserved barriers are generally expressed in the landscape as small ridges (generally less than 1 m in height) covered by shell middens a few dm thick.

This superposition of landforms allows us to use Google Earth satellite imagery as a preliminary tool to locate coastal sand ridges and their shell middens. Hundreds of shell middens appear very clearly on these images, forming a series of nearly continuous ridges (Fig. 2D) from north to south. Their estimated distribution before the field surveys was checked *in situ*, with visual control in some cases to remove doubts. The linear features are identified according to their form and the nature of their constituent materials, as well as their vertical and horizontal dimensions and orientation.

3.2 Ages of paleo-shorelines

To establish the chronology of sand-ridge formation, we take into consideration the data provided by geomorphology, sedimentology and archaeology (Vernet, 1998 and 2007), using a geoarcheological approach for the determination of RSL curves (Brückner, 2005; Ghilardi et al, 2013; Morhange and Marriner, 2015). The radiocarbon dating of *Senilia* valves was

carried out by the Laboratory of Oceanography and Climate (LOCEAN-UMR 7159, at the University Pierre and Marie Curie, Paris) and by the GADAM (Silesian University of Technology, Gliwice, Poland). The dates are calibrated using Marine09 (Reimer et al., 2009). Numerous measurements on samples of continental origin (for example, organic remains in pottery shards contained in shell middens, ostrich eggs, etc.) and *Senilia shells*, lead us to adopt a marine reservoir effect correction (ΔR) of -300 ± 50 years for materials on the foreshore of the BA (Vernet, unpublished data) instead of the value of 70 ± 13 years proposed by Ndeye (2008) for the edge of the BA. Based on these data, we can use the chronological stages in the development of coastal plain sedimentary structures to outline the history of this area. Dia (2013) defined six episodes subdividing the late Holocene of the BA (Table 1). These episodes are separated by short intervals during which no linear sedimentary structures were formed anywhere on a coastal plain almost 300 km long.

3.3 Reconstruction of the topographic elevation of paleo-shorelines

We assume that the dates of the shell middens are coeval with the underlying barriers because Neolithic groups probably occupied these sedimentary structures as soon as they were formed (Barusseau et al., 1995). Thus, the shoreline location at any time in the late Holocene corresponds to the position of the coastal barrier at that time. These characteristic coastal features are made up of mixed sedimentary structures (berms due to wave action and small dunes linked to aeolian transport) delimited at their base by the top of the swash zone. The height of the berm base depends on the maximum elevation of sediment transport during the uprush. Under the highly attenuated wave conditions of the BA, these sedimentary structures are no higher than a few cm or a few dm (<50 cm) above high tide level (HTL), depending on the exposure to waves. Barrier thickness may then increase by the action of the wind; the berm evolves into a ridge or small coastal dune whose base remains

attached to the position of the swash zone. By defining the base of this sedimenary structure, it is possible to describe an index point which provides a reference datum relative to the tide level (Vacchi et al., 2016). According to various authors, it is necessary to establish the precise elevation of a sample attached to an index point to determine the position of relative sea level (RSL) (van de Plassche, 1986; Horton et al., 2000; Woodroffe & Horton, 2005; Barlow and Shennan, 2008; Engelhart et al., 2011; Baeteman et al., 2011). As pointed out by Vacchi et al (2016), to produce an index point, the calibrated age of each sampled RSL marker should be known. Moreover, the marker must be defined in terms of its position in a specific domain of the coastal zone as well as according to elevation in relation to a reference level. The position of the marker in the coastal zone implies applying an estimate of the indicative height range that the marker is likely to occupy. In the case of the BA coastal plain, following Shennan et al. (2006) and Barlow and Shennan (2008), we consider the contact between intertidal and supratidal sediments on a low-energy coast, thus providing valuable sea-level index points. More precisely, we assume that an index point is formed by the contact between barrier base and the sand flat foreshore (Fig. 2C), identified by a varied faunal assemblage. We also base this assumption on Curray et al. (1969), who proposed that coastal features such as beach ridges emerge above sea level during fair weather wave conditions, with the result that they indicate the high tide level. In our case, the indicative range is the swash height (Sh) and the reference level is the lower part of the swash zone, corresponding to the high tide level (HTL) (Fig 3). The high tide level is established from a series of geodetic measurements carried out using a Geodimeter total station along several sectors of the coast, allowing us to define valid sea-level index points on seven profiles in the bays of Aghouenit and Aouatil (Fig. 1). The measurement is first related to the position of the current HTL, and then to the MSL. The HTL is defined by the

263 position of the limit between dry and wet sand; a systematic error of ±0.25 m is applied to
264 the measurement of this mark. The total error on the measurement is estimated by taking
265 into account the quadratic error on the different elements of the calculation: experimental
266 measurement by total station, HTL position and swash amplitude. During these calculations,
267 some barriers are dated using samples from their overlying middens while others are
268 attributed an age based on their attachment to a dated paleo-shoreline.
269
270 **4. Results**
271 In an area as large as the BA coastal plain, it is first necessary to compile the available data
272 to obtain an insight into the general spatial pattern of the sedimentary units. In the
273 following, we qualitatively validate this pattern by supplementing it with the results from
274 many previous studies (Barusseau et al., 2007, 2009 and 2010; Dia, 2013). Our objective is to
275 illustrate how the successive palaeo-shorelines of the late Holocene can be integrated into a
276 simple model which can then be used to link the index points to the changes in sea level
277 defined by a specific RSL curve.
278 **4.1 Spatial and chronological distribution of late Holocene paleo-shorelines of the Banc**
279 **d'Arguin**
280 The extreme flatness of the BA coastal plain is clearly evident throughout its 200-km-long
281 extent from North to South. Indeed, it is difficult to pick out small elevations of 2 to 3 m on
282 the coastal plain, which can reach a width of up to 12 km.
283 However, barriers belonging to different episodes of the late Holocene are sometimes
284 closely spaced together, providing evidence of their position on a sub-horizontal plane. This
285 is the case for the Téchekché barriers (Fig. 4A and B), which form a series of 7 to 8 bars
286 developed during the late Holocene, located at the outlet of a wadi which functioned on

several occasions. According to the cross-section presented in Fig. 4D, the shell middens/ridges that accumulated between 4420 ±90 and 2415 ±105 cal yr BP lie above a basal plane always situated at the same elevation. Furthermore, we apply a WGS 84 Digital Terrain Model with 1-m spaced contours over the entire intertidal zone of the Banc d'Arguin to simulate a 1 m-flood using geo-referenced orthophotos from Google Earth. In the Téchekché-Arguin island-Tintan peninsula sector (Fig. 4C), the entire coastal plain can be invaded by the sea following a very small increase in sea level (1 m), thus confirming the extreme flatness of the area at a regional scale, including all the barrier zones.

4.2 Archaeological evidence

Another set of observations tends to support this view of the distribution of paleo-shorelines. Recent studies have shown the great importance of archaeological remains for reconstructing variations in sea level (Morhange and Marriner, 2015). Indeed, the use of archaeological data in the northern sector of the study area (Bay of Arguin-Tintan) allows us to show that the tidal zone remained in the same position throughout the late Holocene. A large number of fish traps (or weirs) have been identified and mapped on the western foreshore of the Tintan peninsula (Vernet et al., 2011; Vernet, 2014). These Neolithic structures are situated close to bedrock outcrops and are built of rocky slabs. The traps extend in various forms over an area more than 10 km long and 2 km wide at around 20°55'N, 16°43'W (Fig. 5). These traps can only be dated indirectly using results from nearby shell middens, where hearths are found containing abundant fish remains (mainly vertebrae). These remains have been dated at 2790 ± 70 cal yr BP (Vernet, 2014). The disappearance of the Neolithic populations at the end of the middle part of the late Holocene due to aridification explains why no fish traps have been identified with more recent ages.

4.3 Toward a general model

The pattern of shoreline evolution described above can be generalized throughout the Banc d'Arguin, as illustrated in the Iwik peninsula sector (Fig. 6), where there is an succession of alternating sand flats and barriers (beach ridges, coastal dunes, sedimentary spits) formed between 5090 ±200 and 2370 180 cal yr BP. All these landforms are adjusted to the same base level as shown below. As established from the cross-section at Téchekché (Fig. 4D), we can define a conceptual geomorphological model for the development of the BA coastal plain. This model implies a continuous progradation of sand flats and the episodic formation of linear sedimentary units (mean height: approx. 1 m). Although the model remains valid when applied to other parts of the BA, the horizontal scale should be extended since the intervals between barriers are of the order of kilometres while their width is only a few tens of metres. These barriers also contribute to accelerating the progradation since they give rise to a sheltering effect. The beach ridges and middens prograde onto the marine domain over a flat surface, alternating in chronological succession as they advance seaward. Accordingly, by assuming a general and simple model for the development of the coastal plain, we can constrain the elevation of the paleo-shoreline positions using only a small number of cases where the index point is defined by the contact between the prograding sand flat surface and the barrier base.

4.4 Index points

Geodimeter measurements were carried out on 7 profiles to obtain representative index points. Tables 2 and 3 present all the information related to the definition and measurement of the index points. Table 2 provides a detailed description of the situation of the measured index points and the field characteristics. Table 3 summarizes the quantitative results and the corresponding uncertainties. The seven index points selected here correspond to

different morphological situations. The case of IP1 is of special interest because this point is defined in an excavation on the sand flats of Aghouenit bay (Fig. 7A). Extending inland from the head of the bay, the late Holocene interdunal filling forms a horizontal sand flat between two dune ridges (about 15 m high) of the Azéfal Sand Sea, which are capped or bordered by several generations of shell middens dated at between 6510 ± 220 and 3960 ± 110 cal yr BP. Fig. 7C presents the corresponding profile (profile 1) along the axis of the interdune area, showing that, within its overall extent (more than 5 km), the sand flat surface is situated at an elevation of no more than 0.62 m above HTL. Even though greater heights are attained in the two present-day dune and barchan fields, these features have no particular impact on establishing the variations of late Holocene sea level. At the inland extremity of profile 1, a test trench excavated at point 8 indicates the presence of an aeolian red sand layer overlying a sandy deposit with dominant *S. senilis* shells (Nouakchottian beach, 5640 ± 90 yr). The base of this beach deposit overlies a layer containing shell debris and small *Cardium* shells, situated at around - 0.65 m below the surface, i.e. - 0.03 m/HTL (IP1 in table 3). The morphological situation of IP2 (Fig. 6) corresponds to the contact between a sand flat abutting against a sand ridge capped by a midden (early part of late Holocene, 4650 ± 650 yr) and adjacent to the Tafaritian basement. The ridge toe has an elevation of 0.64 m above the current high tide level. IP3 illustrates the typical situation described in Fig. 3; the point is represented by a low-elevation barrier located near the earlymost late Holocene paleo-shoreline. In the other four cases, the barrier is backed by a dune of a variable elevation (IP4, 5, 6 and 7). Figures 7B and D give the location and cross-section for IP5 in profile 2. On the eastern edge of the bay of Aghouenit, the sand flat is never more than a few centimetres above the highest tide level (HTL). A shell midden dated from the middle late Holocene (3200 ± 500 yr - point 5) is located at the toe of an elevated dune capped by a shell midden

(point 12) that was built up when the sea reached the dune during the Nouakchottian stage. The point of contact of the sand flat with the barrier (points 4 and 6 on profile 2) is located at +0.77 m above HTL (IP5 in Table 3). While IP4, 6 and 7 are in a similar morphological situation, their position is not illustrated here. The chronological attribution of IPs is only established in three cases by radiocarbon dating. In all other cases, a relative age is given by assigning the structure underlying the IP to one of the six episodes of the late Holocene (Dia, 2013).

5. Discussion

5.1 Specificity of the BA coastal zone

Even if field work in Mauritania is complicated and our study evidently lacks supplementary data such as measurements from ground-prenetrating radar, the model of construction of the BA coastal zone established here seems robust. It is based on numerous morphological and archeological observations on the whole BA region (200 km). The abundance of shell middens found on the BA allows the measurement of many radiocarbon dates and provides a unique opportunity to recreate the chronological steps of progradation on a very flat surface.

The specific conditions of sedimentation on the BA coastal plain are related to its position at the edge of a large desert with dominant winds blowing towards the sea. This is reflected in the sedimentological characteristics which are marked by a dominance of sand. In low-latitude regions, similar environments are usually characterized by an enhanced development of bio-geochemical sedimentation (Hagan & Logan, 1974; Evans, 2011). The huge amount of sediment supply all along the BA coastline leads to the creation of very extensive and flat coastal plains made up of fine-sand. Even if the rate of shoreline

383 progradation increased during the aridification, it remained spatially uniform over the entire
384 BA region (Dia, 2013), due to the protection offered by shoals on the inner shelf (Aleman et
385 al., 2014) which prevented Atlantic swell from reaching the coastline. In the coastal zone of
386 the BA, the observed longshore drift is generated solely by the wind sea, episodically leading
387 to the formation of barriers.
388 In contrast to many coastal regions where it is a question of establishing a sea-level
389 variation curve for the late Holocene, the desert environment around the Gulf of Arguin
390 does not provide suitable material for analysis so morphological markers are required to
391 resolve the issue. Measured paleo-shoreline levels are found to lie within a few dm of the
392 present sea level since ca 7000 cal yr BP. This implies that the relative sea level in the
393 Mauritanian region oscillated throughout this time interval within the usual range of natural
394 sea-level variations, whereas larger magnitude variations occurred in other regions. In 2010,
395 the present authors observed a storm surge during a summer monsoon episode showing
396 that a marine incursion of shallow water depth can still locally approach the limit of the ca.
397 7000 cal yr BP coastline.
398 **5.2 Index point validity**
399 Various markers are used to define index points relating to relative sea-level during post-
400 glacial and Holocene times. These markers (or sea-level indicators) can be based on biogenic
401 materials including coralline rhodophytes, worm snails Vermetidae, ostracods, diatom or
402 Foraminiferal assemblages, as well as marsh plant macrofossils and marine brackish molluscs
403 (Leorri and Cearreta, 2009; Kemp et al., 2009; Vacchi et al., 2016) or geological samples
404 such as beachrocks with cement fabric (Castro et al., 2014; Vacchi et al., 2016). Sometimes,
405 terrestrial samples such as wood from river banks or basal peat beds provide an upper age
406 limit (Van de Plassche et al., 1998; González and Törnqvist, 2009; Baeteman et al., 2011). In

the BA, such indicators are rare, due to the dominantly sandy facies of the sand flats and barriers. Barriers are mainly unfossiliferous and, with the exception of some sand flats containing fossils in life position, the shells may not be in place.

Alternative proxies such as coastal barrier deposits have also been successfully used to explore variations in sea level (Tamura et al., 2008; Nielsen and Clemmensen, 2009; Billy et al., 2015; Costas et al., 2016). Moreover, subsurface sediment facies boundaries represent useful indicators of sea level, e.g. aeolian and beach sediments (Van Heteren et al., 2000; Billy et al., 2015), as well as sediments on the foreshore and shoreface (Hede et al., 2015) or on the upper and lower shoreface (Tamura, 2012). In this context, on a low-energy coast such as the BA, we may consider that valuable index points can be derived from the contact between intertidal and supratidal sediments (Shennan et al., 2006; Barlow and Shennan, 2008). According to Curray et al (1969), such points indicate the position of high tide level. Therefore, the index points chosen in the BA define the contact between the sand flat and the barrier base (Fig. 3). In most cases, the barrier is at a low elevation (a few tens of cm) above the sand flat. In this region, where the winds are generally strong, barriers are only preserved due to the sheltering effect of shell middens. Such barriers can be reasonably interpreted as berms formed above the upper limit of the swash zone. More rarely, the barrier is of the order of 0.5 to 1 m above the sand flat, and is interpreted as an incipient dune. Exceptionally, the barrier can reach a height of 3 to 5 m, notably in the earlymost late Holocene, in which case it can be interpreted as a foredune (Hesp et al., 2005) formed by aeolian sand deposition. In all three cases, the barrier sole is adjusted to the upper limit of the berm uprush. This qualitative attribution is used here for the definition of index points. However, uncertainties arises in the evaluation of the amplitude of the swash. The height of the measured point represents the elevation of the swash zone at the highest sea level

(HTL), at the time of deposition of the barriers. The indicative range in elevation of the barrier above the sand flat is then estimated in relation to the morphological position of the IP, and particularly its exposure to waves. Several factors related to the exposure of the coast to waves are taken into account. In the Bay of Aouatil (IP2 and 3), the sheltering effect of the Iwik Peninsula gives rise to refraction and consequent attenuation of the waves (Barusseau et al., 2009); the indicative height range is established at 0.25 ±0.2 m. The coastal environment is much more sheltered in the bay of Aghouenit, which is largely unaffected by wave action (Fig. 1); the indicative height range is established at 0.15 ±0.1 m (IP4, 5, 6 and 7) and even 0.1 ±0.1 m for the point furthest inland from the inlet (IP1 - Fig. 7A).

We also discuss here the problem of attributing ages to the index points. Indeed, we assume that dating a shell midden allows us to attribute an age to the underlying sedimentary structure. There are two reasons justifying this assumption. Firstly, coastal features in the BA region are very rapidly formed. Over the entire length of the BA coast, barriers may be considered to be of the same age. This is due to the abundance of available sandy material. Secondly, faced with the need to prepare food for consumption, human groups harvesting *Senilia* in the intertidal zone would be expected to use fire to open the shells. It is legitimate to consider that these groups would make use of the sedimentary relief closest to areas sheltered from the tide.

For the reasons explained above, the RSL curve presented here shows that sea level has remained close to the present-day position since the beginning of the late Holocene (Fig. 8). The measurements indicate that sea-level variations since at least 5000 yrs BP have remained mainly within the current tidal range. This particular pattern of sea-level change in the late Holocene is responsible for the spreading of surface sedimentary units over the coastal zone adjoining the BA.

455 Finally, the association of morphosedimentary and archaeological data leads us to infer
456 that the relative sea level was fairly stable in this area during the late Holocene, thus
457 validating the RSL curve between 6600 and 1400 cal yr BP (Fig. 9). This curve shows
458 fluctuations around the zero chart datum, with a range of variations consistent with the
459 natural changes of sea level, even if limited oscillations of amplitude lower than 1 m cannot
460 be ruled out. The proposed curve is completely different from that previously accepted for
461 the region (Einsele et al., 1974). There is no significant rise in sea level above +2 m and no
462 fall below -3 m.

463 **5.3 Comparison of RSL curves between the BA and other low-latitude regions**

464 The late Holocene RSL changes in the BA should be confronted with situations observed in
465 other regions of the world in similar latitude bands (low and mid-latitude) or the same
466 geophysical setting (Clark zones III and IV). Recent studies discuss these issues in the Gulf of
467 Mexico, on the coasts of Brazil, South Africa, Australia and Vietnam as well as some oceanic
468 islands (table 4).

469 All these regions exhibit a varied but persistent rise of sea level above its present-day
470 datum. The highstand varies between ca. + 1/+2 m (Gulf of Mexico, Brazil coast, New South
471 Wales and south coast of Western Australia,Vietnam, Hawaii) and + 4.5 m (South Australia
472 and Tasmania). Generally speaking, the sea level falls more or less regularly after the
473 highstand. In South Africa, episodes of alternating rise and fall are observed which are due to
474 minor isostatic movements. By contrast, the BA shows a simpler RSL curve which appears to
475 reflect a particularly unusual situation, with no marked highstand and a lack of successive
476 movements of rise and fall. What are the possible causes for such a difference?

477

478

5.4 Possible explanations of the RSL curve in the Banc d'Arguin region

In the following, we review the role of various factors affecting the pattern of late Holocene sea-level change in the study area, analysing those factors which play a major role and, finally, considering the possible influence of causes hitherto neglected.

As noted above, the local RSL curve should be corrected for disturbing mechanisms: local disturbances, tectonic instability, impact of crustal compensation and isostatic processes. In the BA, local factors have no impact on the variation of sea level. Indeed, the major input of aeolian dust during the middle-late Holocene (Dia, 2013) only influences the progradation. Since the Senegal-Mauritanian Meso-Cenozoic sedimentary basin is located on the northwestern margin of the African craton, the region is tectonically stable for several reasons. First, this sedimentary basin abuts against the Reguibat shield and the Archean Amsaga nucleus (Trompette 1973; Cahen et al., 1984; Potrel et al., 1996; Chardon 1997, Chakiri et al., 2014) which form a rigid bedrock (Block, 2015). Then, subsidence in the basin ceased from Cenomano-Turonian times onward (Ndiaye, 2012). Third, the BA is far away from the subsident delta of the Senegal River (Monteillet et al., 1981; Monteillet, 1986) and also from the zone of weak seismic activity at the boundary of the Reguibat shield and the Taoudeni basin (http://sismique.zone/mauritanie,22/01/2016). The resulting stability counteracts the influence of continental flexure by preventing the hydro-isostatic effect of crustal subsidence on the oceanward side (Mitrovica and Milne, 2002) and the symmetrical upwarping by leverage on the continental side (Walcott, 1972; Clark et al., 1978; Nakada and Lambeck, 1989). Moreover, in the geophysical model of Clark et al. (1978), Mauritania is located near the boundary between zones III and IV. Thus, the tendency towards the emergence of zone III can offset the tendency to submergence of zone IV, leading to a restriction of the vertical movements of the RSL.

503 Under these conditions, ocean syphoning (Mitrovica and Peltier, 1991; Mitrovica and
504 Milne, 2002) should be a dominant factor. By increasing the accommodation potential of the
505 ocean floor due to forebulge collapse, this mechanism leads to a lowering of sea level
506 throughout the oceanic domain. This phenomenon is particularly evident in oceanic islands
507 where variable effects are observed (Woodroffe and McLean, 1990, Grossman and Fletcher,
508 1998, Nunn and Peltier, 2001, Woodroffe and Horton, 2005), as well as in intertropical zones
509 (Statteger et al., 2013). In this way, ocean syphoning would be responsible for the
510 subsequent fall observed after the highstand episode (Table 4). In the case of the BA, where
511 such a fall is not observed, we need to consider another cause for this compensation
512 mechanism. Since the volume deficiency caused by ocean syphoning can only be
513 counteracted by water input, this raises the question of the continuation of glacial melting
514 throughout the late Holocene.
515 Glacial melting is punctuated by meltwater pulses (Edwards, 2005; Woodroffe and Horton,
516 2005). The most recent recorded pulse occurred around 7,000 / 8,000 years BP (Milne et al.,
517 2005, Milne and Mitrovica, 2008). However, the date of cessation of ice sheet melting is a
518 matter of debate: estimates range from 6,000-5,000 years BP (Lambeck and Nakada, 1990;
519 Lambeck et al., 2014), 4,000 years BP (Nunn and Peltier, 2001; Mason and Jordan, 2002;
520 Milne et al., 2005; Engelhart et al., 2009), around 2000-1000 years (Fleming et al., 1998), up
521 to the present (Lambeck and Nakada, 1990). This last hypothesis is supported by the
522 observation of a stable relative sea level in the BA zone, and supports the idea of a
523 significant prolongation of glacial retreat after 6000/5000 years BP. At least, the intensity
524 and duration of glacier melting remains an unresolved issue. As pointed out by Gehrels
525 (2010), monitoring ice melting during the late Holocene will be an important aspect of future
526 research.

6. **Conclusion**

Successive barrier beaches accumulated during the late Holocene on the coastal sand-flats of the Banc d'Arguin, which form a topographically planar and regular surface. This climate-driven spatial pattern reflects a rather stable sea level in this region between 6500 cal yr BP and the present day. This stability is inferred from the measured elevation of index points distributed throughout the late Holocene. The index points used here are defined in relation to the position of the barrier sole, adjusted to the upper limit of the berm uprush. The elevations of these index points are measured by total station. Measurements show that changes in sea level during the late Holocene do not exceed the present-day natural variations observed in the marine environment (tides, swell, monsoon storm surges, etc.). The pattern of late Holocene RSL changes in the BA is different from variations observed in comparable low-latitude regions elsewhere in the world, where the sea level generally falls more or less regularly after a highstand. By contrast, the simpler RSL curve of the BA appears particularly unusual, with no marked highstand and the absence of any successive movements of rise or fall. Among the causes usually evoked to explain RSL changes, local factors and tectonic instability can be ruled out for this part of Mauritania. Therefore, in areas far away from centres of deglaciation, we would expect to observe a lowering of sea level due to ocean syphoning. The lack of such an effect implies compensation by a rise in sea-level of a similar order of magnitude. As a result, we propose that ice sheet melting continued throughout the late Holocene, as sometimes evoked in the literature.

551

552 **Acknowledgments**

553

554 This research was supported by the programme PACOBA (Programme d'Amélioration des
555 COnnaissances du BA) and funded by the French Ministry of Foreign Affairs. IMROP and
556 PNBA are thanked for their logistic support. The assistance of Pierre Labrosse, an IMROP aid
557 worker, is also acknowledged. We also would like to thank four anonymous reviewers and
558 the editor Nicholas Lancaster for providing constructive suggestions and comments that
559 have helped to improve this paper. Michael Carpenter post-edited the English style and
560 grammar.

561

562 **References**

563

564 Aleman, N., Certain, R., Barusseau, J.-P., Courp, T., Dia, A., 2014. Post-glacial filling of a
565 semi-enclosed basin: The Arguin Basin (Mauritania). Marine Geology, 349, 126-135.
566 Angulo, R.J., Lessa, G.C., Souza, M.C., 2006. A critical review of the Mid- to Late Holocene
567 sea-level fluctuations on the eastern Brazilian coastline. Quaternary Science Reviews 25,
568 486–506.
569 Baeteman, C., Waller, M., Kiden, P., 2011. Reconstructing middle to late Holocene sea-level
570 change: A methodological review with particular reference to 'A new Holocene sea-level
571 curve for the southern North Sea' presented by K.-E. Behre. Boreas 40, 557-572.
572 Barlow, N.L.M., Shennan, I., 2008. An Overview of Holocene Coastal Change From Berwick-
573 upon-Tweed to Whitby. In: Tolan-Smith, C., North East Rapid Coastal Zone Assessment
574 (NERCZA). Archaeological Research Services Ltd and English Heritage, 19-41.

575 Barusseau, J.-P., Bä, M., Descamps, C., Diop, S., Giresse, P., Saos, J.-L., 1995. Coastal
576 evolution in Senegal and Mauritania at 10^3, 10^2 and 10^1 year scales: Natural and human
577 records. Quaternary International 29-30, 61-73.
578 Barusseau, J.-P., Vernet, R., Saliège, J.-F., Descamps, C., 2007. Late Holocene sedimentary
579 forcing and human settlements in the Jerf el Oustani - Ras el Sass region (Banc d'Arguin,
580 Mauritania). Géomorphologie 7, 7-18.
581 Barusseau, J.-P., Certain, R., Vernet, R., Saliege, J.-F., 2009. Morphosedimentological record
582 and human settlements as indicators of West-African Late Holocene climate variations in the
583 littoral zone of the Iwik peninsula (Banc d'Arguin - Mauritania). Bulletin de la Societe
584 Geologique de France 180, 449-456.
585 Barusseau, J.-P., Certain, R., Vernet, R., Saliège, J.-F., 2010. Late Holocene morphodynamics
586 in the littoral zone of the Iwik Peninsula area (Banc d'Arguin - Mauritania). Geomorphology
587 121, 358-369.
588 Billy, J**.,** Robin, N., Hein, C., Certain, R. & Fitzgerald D, D., 2015. Geo-chronological pattern
589 of a periglaciaire beach-ridge plain formation, the Miquelon-Langlade Barrier in NW Atlantic,
590 Geomorphology, Vol. 248, 134-146.
591 Block, S., Ganne, J., Baratoux, L., Zeh, A., Parra, L.A., Jessell, M., Ailleres, L., and Siebenaller,
592 L. (2015). Petrological and geochronological constraints on lower crust exhumation during
593 paleoproterozoic (eburnean) orogeny, NW Ghana, West African craton. Journal of
594 Metamorphic Geology, 33 (5), 463-494.
595 Brückner, H., 2005. Holocene shoreline displacements and their consequences for human
596 societies: the example of Ephesus in western Turkey. In: Fouache, E., Pavlopoulos, K., (Eds.),
597 Sea Level Changes in Eastern Mediterranean during Holocene Indicators and Human
598 Impacts, Zeitschrift für Geomorphologie, Supplementbände 137, 11-22.

599 Cahen, L., Snelling, N.J., Delhal, J., Vail J.R., 1984. The geochronology and evolution of the
600 Africa. Clarendon Press, Oxford, 512 p.
601 Castro, J. W. A., Suguio, K., Seoane, J. C.S., Da Cunha, A. M. and Dias, F. F. 2014. Sea-level
602 fluctuations and coastal evolution in the state of Rio de Janeiro, southeastern Brazil. Anais da
603 Academia Brasileira de Ciências, 86, 2, 671-683.
604 Chakiri, A.H.S., El Hadi, H., Baghdad, B., Zahidi, K., 2014. Etude géochimique de la
605 minéralisation polymétallique de la zone de l'Amsaga (Dorsale de Rgueïbat, Mauritanie).
606 European Scientific Journal 10 (21), 86-100.
607 Chardon, D., 1997. Les déformations continentales archéennes. Exemples naturels et
608 modélisation thermomécanique. PhD Thesis, University of Rennes, 257 p.
609 Clark, J.A., Farrell, W.E., Peltier, W.R., 1978. Global Changes in Postglacial Sea Level: A
610 Numerical Calculation. Quaternary Research 9, 265-281.
611 Costas, S., Ferreira O., Plomaritis, T.A. and Leorri E., 2016. Coastal barrier stratigraphy for
612 Holocene high-resolution sea-level reconstruction. Sci. Rep. 6,
613 38726.doi :10.1038/srep38726.
614 Curray, J.R., Emmel, F.J., Crampton, P.J.S., 1969. Holocene history of a strand plain,
615 lagoonal coast, Nayarit, Mexico. In: Castanares, A.A., Phleger, F.B. (Eds), Coastal lagoons, a
616 Symposium. Mexico, Unam-Unesco, 1967, p. 63-100.
617 Descamps, C., Thilmans, G., Thommeret, Y., 1974. Données sur l'édification de l'amas
618 coquillier de Dioron-Boumak (Sénégal). ASEQUA 41, 67-83.
619 Dia, A., 2013. Les plateformes littorales des marges stables désertiques : Etude
620 sédimentologique, stratigraphique et morphologique des unités fini-holocènes (=
621 Néholocène) du Banc d'Arguin (Mauritanie). Unpublished thesis, Universty of Perpignan Via
622 Domitia, France, 213 p.

623 Edwards, R., 2005. Sea levels: abrupt events and mechanisms of change. Progress in
624 Physical Geography 29 (4), 599-608.
625 Einsele, G., Herm, D., Schwarz, H.U., 1974. Sea level fluctuation during the past 6000 yr at
626 the coast of Mauritania. Quaternary Research 4, 282-289.
627 Einsele, G., Elouard, P., Herm, D., Kögler, F.C., Schwartz, H.U., 1977. Source and biofacies of
628 Late Quaternary sediments in relation to sea level on the shelf off Mauritania, West Africa.
629 "Meteor" Forsch. Ergebnisse C (26), 1-43.
630 Elouard, P., 1975. Formations sédimentaires de Mauritanie atlantique. In : Monographies
631 géologiques régionales : Notice explicative de la carte géologique au 1/1000000 de la
632 Mauritanie, BRGM, Paris, 171-254.
633 Engelhart, S.E., Horton, B.P., Douglas, B.C., Peltier, W.R., Tornqvist, T.E., 2009. Spatial
634 variability of late Holocene and 20th century sea-level rise along the Atlantic coast of the
635 United States. Geology 37, 1115-1118.
636 Engelhart, S.E., Horton, B.P., Kemp, A.C., 2011. Holocene sea level changes along the
637 United States' Atlantic Coast. Oceanography 24 (2), 70-79.
638 Evans, G. 2011. An historical review of the Quaternary sedimentology of the Gulf
639 (Arabian/Persian Gulf) and its geologic impact. In: Kendall, C.G.St.C., Alsharhan, A.S., Jarvis, .,
640 Stevens, T. (Eds.), Quaternary carbonate and evaporite sedimentary facies and their ancient
641 analogues: a tribute to Douglas James Shearman, Special publication 43 of the International
642 Association ofSedimentologists, Wiley-Blackwel, 11-44.
643 Faure, H., Elouard, P., 1967. Schéma des variations du niveau de l'océan Atlantique sur la
644 côte de l'Ouest de l'Afrique depuis 4000 ans. C.R. Acad. Sci. Paris D (265), 784-787.

645 Faure, H., Fontes, J.C., Hebrard, L., Monteillet, J., Pirzzoli, P.A., 1980. Geoidal changes and
646 shore level tilt along Holocene estuaries: Senegal River area, West Africa. Science 210, 421-
647 423.
648 FitzGerald, D.M. and Buynevich, I.V. 2005. Coastal Barriers. In: Encyclopedia of Life Support
649 Systems, UNESCO-EOLSS Publishers Co, Ltd.
650 Fleming, K., Johnston, P., Zwartz, D., Yokoyama, Y., Lambeck, K., Chappell, J., 1998. Refining
651 the eustatic sea level curve since Last Glacial Maximum using far-intermediate field sites.
652 Earth and Planetary Science Letters 163, 327-342.
653 Gehrels, R. 2010. Sea-level changes since the Last Glacial Maximum: an appraisal of the
654 IPCC Fourth Assessment Report. J. Quaternary Sci., Vol. 25 pp. 26–38.
655 Ghilardi, M., Colleu, M., Pavlopoulos, K., Fachard, S., Psomiadis, D., Rochette, P., Demory,
656 F., Knodell, A., Triantaphyllou, M., Delanghe-Sabatier, D., Bicket A. and Fleury, J. 2013.
657 Geoarchaeology of Ancient Aulis (Boeotia, Central Greece): human occupation and Holocene
658 landscape changes Journal of Archaeological. Science, 40, 2071-2083.
659 González, J.L., Törnqvist, T.E., 2009. A new Late Holocene sea-level record from the
660 Mississippi Delta: evidence for a climate/sea level connection? Quaternary Science Reviews
661 28, 1737-1749.
662 Grossman EE, Fletcher CH (1998) Sea level higher than present 3500 years ago on the
663 northern main Hawaiian Islands. Geology 26:363–366.
664 Hagan, G.M. and Logan, B.W. 1974. History of Hutchison embayment tidal flat, Shark Bay,
665 Western Australia. American Association of Petroleum Geologists, Tulsa, Oklahoma, U.S.A.,
666 Memoir 22, 283-315.

667 Hamoud, A., El Hadi, H., Chakiri, S. and Tahiri, A. 2015. Caractérisation pétrographique et
668 géochimique des métabasites archéennes d'Amsaga Est (Dorsale de Rgueïbat, Mauritanie).
669 European Journal of Scientific Research, 135, 3, 228-242.
670 Hébrard, L., 1973. Contribution à l'étude géologique du Quaternaire du littoral mauritanien
671 entre Nouakchott et Nouadhibou. (18°-21° lat. N). PhD Thesis, University of Lyon, 549 p.
672 Hede M.E., Sander L., Clemmensen L. B., Kroon A., Pejrup M., Lars Nielsen. 2015. Changes
673 in Holocene relative sea-level and coastal morphology: A study of a raised beach ridge
674 system on Samsø, southwest Scandinavia. The Anthropocene Review, 25, 9, 1402-1414.
675 Horton, B.P., Edwards, R.J., Lloyd, J.M., 2000. Implications of a microfossil transfer function
676 in Holocene sea level studies. In: Shennan, I., Andrews, J., (Eds.), Holocene land-ocean
677 interaction and environmental change around the North Sea. Geological Society, London.
678 Special Publications 166, pp. 275-288.
679 Kelletat, D., 2005. A Holocene sea level curve for the eastern Mediterranean from multiple
680 indicators (with 4 figures). In: Fouache, E., Pavlopoulos, K., (Eds.), Sea Level Changes in
681 Eastern Mediterranean during Holocene Indicators and Human Impacts, Zeitschrift für
682 Geomorphologie, Supplementbände 137, 1-9.
683 Kemp A.C., Horton B.P. and Culver S.J. 2009. Distribution of modern salt-marsh
684 foraminifera in the Albemarle-Pamlico estuarine system of North Carolina, USA: Implications
685 for sea-level research. Mar. Micropaleontol., 72, 222–238.
686 Lambeck, K., Nakada, M., 1990. Late Pleistocene and Holocene sea-level change along the
687 Australian coast. Palaeogeography, Palaeoclimatology, Palaeoecology 89, 143-176.
688 Lambeck, K., Purcell, A., Johnston, P., Nakada, M., Yokoyama, Y., 2003. Water-load
689 definition in the glacio–hydro–isostatic sea-level equation. Quaternary Science Reviews 22
690 (2-4), 309-318.

691 Lambeck K., Rouby H., Purcell A., Sun Y., and Sambridge M. 2014. Sea level and global ice
692 volumes from the Last Glacial Maximum to the Holocene. PNAS, 111, 43, 15296-15333.
693 Lancaster, N., Kocurek, G., Singhvi, A., Pandey, V., Deynoux, M., Ghienne, J.-F., Lô, K., 2002.
694 Late Pleistocene and Holocene dune activity and wind regimes in the western Sahara desert
695 of Mauritania. Geology 30, 991-994.
696 Lavaud, R., Thebault, J., Lorrain, A., Van der Geest, M., Chauvaud, L., 2013. Senilia senilis
697 (Linnaeus, 1758), a biogenic archive of environmental conditions on the Banc d'Arguin
698 (Mauritania). Journal of Sea Research 76, 61-72.
699 Leorri E. and Cearreta A. 2009. Recent sea-level changes in the southern Bay of Biscay:
700 transfer function reconstructions from salt-marshes compared with instrumental data.
701 Scientia Marina, 73, 2, 287-296. doi: 10.3989/scimar.2009.73n2287
702 Lézine, A.M., Hély, C., Grenier, C., Braconnot, P. and Krinner, G. 2011 Sahara and Sahel
703 vulnerability to climate changes, lessons from Holocene hydrological data. Quaternary
704 Science Reviews, 30, 3001-3012.
705 Mason, O.K., Jordan, J.W., 2002. Minimal late Holocene sea level rise in the Chukchi Sea:
706 arctic insensitivity to global change? Global and Planetary changes 32, 13-23.
707 Milne, G.A., Mitrovica, J.X., 2008. Searching for eustasy in deglacial sea-level histories.
708 Quaternary Science Reviews 27, 2292–2302.
709 Milne, G.A., Long, A.J., Bassett, S.E., 2005. Modelling Holocene relative sea-level
710 observations from the Caribbean and South America. Quaternary Science Reviews 24, 1183-
711 1202.
712 Mitrovica, J.X., 2003. Recent controversies in predicting post-glacial sea-level change.
713 Quaternary Science Reviews 22 (2-4), 127–133.

714 Mitronica, J.X., Peltier, W.R., 1991. On postglacial geoid subsidence over the Equatorial
715 oceans. Journal of Geophysical Research 96 (B12), 20053-20071.
716 Mitrovica, J.X., Milne, G.A., 2002. On the origin of late Holocene sea-level highstands within
717 equatorial ocean basins. Quaternary Science Reviews 21(20-22), 2179-2190.
718 Monteillet, J., 1986. Évolution quaternaire d'un écosystème fluvio-marin tropical de marge
719 passive: environnements sédimentaires et paléoécologie du delta et de la basse vallée du
720 fleuve Sénégal depuis environ 100 000 ans. PhD Thesis, University of Perpignan, 264 p.
721 Monteillet, J., Faure, H., Pirazzoli, P.A., Ravise, A., 1981. L'invasion saline du Ferlo Sénégal à
722 l'Holocène supérieur 1900 BP. Palaeoecology of Africa and the Surrounding Islands 13, 205-
723 215.
724 Morhange, C. and Marriner, N. 2015. Archeological and biological relative sea-level
725 indicators. *Handbook of Sea-Level Research*, First Edition. Edited by Ian Shennan, Antony J.
726 Long, and Benjamin P. Horton. © 2015 John Wiley & Sons, Ltd. Published 2015 by John Wiley
727 & Sons, Ltd. Chapter 9, 146-156.
728 Nakada, M., Lambeck, K., 1989. Late Pleistocene and Holocene sea-level change in the
729 Australian region and mantle rheology. Geophys. J. 96, 497-517.
730 Ndeye, M., 2008. Marine reservoir ages in Northern Senegal and Mauritania coastal waters.
731 Radiocarbon 50, 281-288.
732 Ndiaye, M., 2012. Etude sismostratigraphique et sédimentologique du Bassin Sénégalo-
733 Mauritanien dans le secteur de Diourbel et Thiès. PhD Thesis, University of Genève, 175 p.
734 Nielsen L., Clemmensen L.B. 2009. Sea-level markers identified in ground-penetrating radar
735 data collected across a modern beach ridge system in a microtidal regime. Terra Nova 21:
736 474– 479.

737 Nunn, P.D., Peltier ,W.R., 2001. Far-field test of the ICE-4G model of global isostatic
738 response to deglaciation using empirical and theoretical Holocene sea-level reconstructions
739 for the Fiji Islands, Southwestern Pacific. Quaternary Research 55, 203-214.
740 Peltier, W.R., 2002. On eustatic sea level history: Last Glacial Maximum to Holocene.
741 Quaternary Science Review 21, 377-396.
742 Pirazzoli, P., 1991. World atlas of Holocene sea-level changes. Oceanography Series 58,
743 Elsevier, Amsterdam.
744 Potrel, A., 1994. Evolution tectono-métamorphique d'un segment de croûte continentale
745 archéenne : Exemple de l'Amsaga (R.I. de Mauritanie), Dorsale Reguibat (Craton ouest
746 africain). Unpublished thesis, University of Rennes 1, France, 414 p.
747 Potrel, A., Peucat, J.J., Fanning, C.M., Auvray, B., Burg, J.P., Caruba, C., 1996. 3.5 Ga old
748 terranes in the west African craton, Mauritania. Journal of the Geological Society 153(4),
749 507-510.
750 Potrel, A., Peucat, J.J., Fanning, C.M. 1998. Archean crustal evolution of the west African
751 craton: example of the Amsaga area (Rgueïbat rise). U–Pb and Sm–Nd evidence for crustal
752 growth and recycling. *Precambrian Research,* 90, pp.107-117
753 Reimer, P.J., Baillie, M.G.L., Bard, E., Bayliss, A., Beck, J.W., Blackwell, P.G., Bronk, Ramsey,
754 C., Buck, C.E., Burr, G.S., Edwards, R.L., Friedrich, M., Grootes, P.M., Guilderson, T.P., Hajdas,
755 I., Heaton, T.J., Hogg, A.G., Hughen, K.A., Kaiser, K.F., Kromer, B., McCormac, F.G., Manning,
756 S.W., Reimer, R.W., Richards, D.A., Southon, J.R., Talamo, S., Turney, C.S.M., van der Plicht,
757 J., Weyhenmeyer, C.E., 2009. IntCal09 and Marine09 radiocarbon age calibration curves, 0-
758 50,000 years cal BP. Radiocarbon 51(4):1111-50.
759 Shennan, I., Horton, B.P., 2002. Holocene land- and sea-level changes in Great Britain.
760 Journal of Quaternary Science 17, 511-526.

761 Shennan, I., Bradley, S., Milne, G., Brooks, A., Bassett, S., Hamilton, S., 2006. Relative sea-
762 level changes, glacial isostatic modelling and ice-sheet reconstructions from the British Isles
763 since the Last Glacial Maximum. Journal of Quaternary Science 21 (6), 585-599.
764 Shennan, I., Milne, G., Bradley, S., 2009. Late Holocene relative land- and sea-level changes:
765 Providing information for stakeholders. GSA Todays 19 (9), 52-53.
766 Skonieczny, C., Paillou, P., Bory, A., Bayon, G., Biscara, L., Crosta, X., Eynaud, F., Malaize, B.,
767 Revel, M., Aleman, N., Barusseau, J.-P., Vernet, R., Lopez, S., Grousset, F., 2015. African
768 humid periods triggered the reactivation of a large river system in Western Sahara. Nature
769 Communications 6:8751.
770 Sloss, C. R., Murray-Wallace, C.V., Jones, B.G., 2007. Holocene sea-level change on the
771 southeast coast of Australia: a review. The Holocene 17 (7), 999-1014.
772 Sloss, C. R., Shepherd, M. & Hesp, P. 2012. Coastal Dunes: Geomorphology. Nature
773 Education Knowledge, 3, 10, 2.
774 Stattegger, K., Tjallingii, R., Saito, Y., Michelli, M., Thanh, T.N., Wetzel, A., 2013. Mid to late
775 Holocene sea-level reconstruction of Southeast Vietnam using beachrock and beach-ridge
776 deposits. Global and Planetary Change 110, 214-222.
777 Tamisiea, M.E., Mitrovica, J.X., 2011. The moving boundaries of sea level change:
778 Understanding the origins of geographic variability. Oceanography 24 (2), 24-39.
779 Tamura T. 2012. Beach ridges and prograded beach deposits as paleoenvironment record.
780 Earth-Science Review, 11, 279-297.
781 Tamura T., Murakami F., Nanayama F. 2008. Ground-penetrating radar profiles of Holocene
782 raised-beach deposits in the Kujukuri strand plain, Pacific coast of eastern Japan. Marine
783 Geology, 248, 11–27.

784 Thomas, Y.F., Senhoury, El M.A., 2007. Distribution de la hauteur significative des vagues
785 significative en Afrique de l'Ouest mesurée par radiomètre Topex–Poséidon. Photo-
786 Interprétation : European Journal of Applied Remote Sensing 2007 (1), 1-24.
787 Trompette, R., 1973. Le Précambrien supérieur et le Paléozoïque inférieur de l'Adrar de
788 Mauritanie (bordure occidentale du bassin de Taoudeni, Afrique de l'Ouest), un exemple de
789 sédimentation de craton. Etude stratigraphique et sédimentologique. University of Provence
790 - Aix-Marseille I, 691 p.
791 Vacchi, M., Marriner, N., Morhange, C., Spada, G., Fontana, A. and Rovere, A. 2016.
792 Multiproxy assessment of Holocene relative sea-level changes in the western
793 Mediterranean: Sea-level variability and improvements in the definition of the isostatic
794 signal. Earth-Science Reviews, 155, 172–197.
795 Van de Plassche, O., 1986. Sea level research: a manual for the collection and evaluation of
796 data. Geo Books, Norwich, U.K., 618 p.
797 Van de Plassche, O., van der Borg, K., de Jong, A.F.M., 1998. Sea-level climate correlations
798 during the past 1400 yr. Geology 26, 319–322.
799 Van Heteren, S., Huntley, D.J., van de Plassche, O., Lubberts, R.K., 2000. Optical dating of
800 dune sand for the study of sea-level change. Geology 28, 411–414.
801 Vernet, R., 1998. Le littoral du Sahara atlantique mauritanien au Néolithique. Sahara 10,
802 21-30.
803 Vernet, R., 2007. Le golfe d'Arguin de la Préhistoire à l'Histoire: littoral et plaines
804 intérieures. Collection PNBA 3, 203 p.
805 Vernet, R., 2014. L'exploitation ancienne des ressources du littoral atlantique mauritanien
806 (7500-1000 cal BP). In : Archéologie des chasseurs-cueilleurs maritimes : de la fonction des

habitats à l'organisation spatiale de l'espace littoral. Séance de la Société Préhistorique Française, Rennes, France, 10-11 April 2014.

Vernet, R., Barusseau, J.-P., Certain, R., Dia, A., 2011. Les barrages à poisson de l'est de la presqu'ile de Tintan (Mauritanie). Proceeding of Colloque international « Anciens peuplements littoraux et relations Homme/Milieu sur les côtes de l'Europe atlantique », september 27th - october 1st, Vannes, France.

Vörösrmarty, C.J., Fekete, B.M., Meybeck, M., Lammers, R.B., 2000. Global system of rivers: Its role in organizing continental land mass and defining land-to-ocean linkages. Global Biochemical Cycle 2 (14), 599-621.

Walcott, R.I., 1972. Past sea levels, eustasy and the deformation of the earth. Quaternary Research 2, 1-14.

Wanner, H., Beer, J., Bütikofer, J., Crowley, T.J., Cubasch, U., Flückiger, J., Goosse, H., Grosjean, M., Joos, F., Kaplan, J.O., Küttel, M., Müller, S.A., Prentice, I.C., Solomina, O., Stocker, T.F., Tarasov, P., Wagner, M., Widmann, M., 2008. Mid- to Late Holocene climate change: an overview. Quaternary Science Review 27, 1791-1828.

Woodroffe, C.D., Mc Lean, R., 1990. Microatolls and recent sea-level change on coral atolls. Nature 344, 531-534.

Woodroffe, S.A., Horton, B P., 2005. Holocene sea-level changes in the Indo-Pacific. Journal of Asian Earth Sciences 25 (1), 29-43.

Figures

Figure 1: On the right, Satellite image of the Gulf of Arguin (©Google Earth). The red dotted frame borders and red dots indicate the positions of the figures and photographs described in the text. On the left, Distribution of zones characterized by particular types of relative sea-level rise during the late Holocene (modified after Clark et al., 1978 and Woodroffe and Horton, 2005). The shape of the characteristic curve is indicated for zones III, IV, V and VI, the only relevant zones in the framework of this study. The localization of zone VI, confined to certain coastal margins (see text), is not indicated.

Figure 2: Geomorphological characteristics of the coastal plain: (A) Photo of the coastal plain between Iwik and Ras Tafarit (20°02.138'N, 16°12.284'W). In the foreground, the edge of the Tafaritian bedrock forms weakly marked relief. Towards the sea, lying on top of older sedimentary units, white patches correspond to shell middens dating back to 5525 ± 55 (1) and 4140 ± 90 cal yr BP (2), respectively. Thumbnail image shows the bottom of foreshore bordering a shell midden topping a sandspit. Proximity to a shell midden is indicated by scattered Senilia senilis *shells and a Neolithic pottery shard. (B) Marine incursion of more than 4 km in an interdune depression, following a monsoon storm in 2010. (C). Shell middens on dune ridges in the south-eastern part of the Tanoudert coastal plain. (D) Satellite image showing same sand barrier as on figure 2C (©Google Earth - 23/2/2003 - 20°19.60'N, 16°15.29'W).*

Figure 3: (A) Schematic representation of the morphological relation between barrier and sand flat.The irregular line forms the sole of the barrier slightly above the high tide level

(HTL). (B) Aspect of the sand flat. (C) Aspect of a barrier forming a low elevation above the sand flat. (D) Position of the barrier sole related to the swash zone. (E) Aspect of the contact between sand flat and barrier.

Figure 4: (A) A series of 7 to 8 mouth bars in three groups developed during the late Holocene, at the outlet of Téchekché wadi lined by the Nouakchottian paleo-shoreline (black line). (B) Photo of the barriers of Téchekché taken from the Pleistocene outcrops. Barriers are represented by white marks lying on the sand flat (C) Simulation showing that the entire zone can be invaded by the sea (blue color) in the event of a very small increase in sea level (1 m); red frame : the zone of the mouth bars of Téchekché. (D) Diagrammatic sketch of the arrangement of successive dated barriers on sand flats accreted during extension of the late Holocene coastal plain, abutting the Tafaritian cliff (on right). This pattern is evocative of the situation encountered at Téchekché.

Figure 5: Neolithic fish traps. The black line marks the limit reached by the Nouakchottian Sea at the end of its rise towards 5500-6000 cal yr BP, the dark-blue line corresponds to the high water mark and the light-blue line to the low tide mark at the time of construction of the fish traps, around 3000 cal yr BP. The zoom view on Fig. 7B allows identification of the fish traps on a photo taken from a kite.

Figure 6: Formation of the Iwik peninsula with the successive positions of late Holocene paleo-shorelines. The Iwik island was incorporated to the land recently after a long period (middle and recent late Holocene) of sandspit construction (Nouakchottian to early late Holocene).Two index points used to calibrate the RSL curve are indicated.

Figure 7: Location and topographic profiles illustrating the measurement of sea level index points in the Aghouenit bay (IP 1: A and B; IP 5: C and D). Description of the profiles is given in table 3. HTL: Current high tide level

Figure 8: Relation between measured elevations, their margins of error and bench marks of present-day sea level: tidal range (lower grey band) and highest sea levels during monsoon (upper light-grey band at top). The index points refer to results given in Table 4 (IP1: Nouakchottian; IP2 and 3: Early late Holocene; IP4, 5 and 6: Middle late Holocene; IP7: Recent late Holocene).

Figure 9: Sea-level rise curve for the Banc d'Arguin. The selected curve shows that the mean sea level (thick curve) attains a value near the current zero chart datum at around 6 500-6 000 years BP. It is accepted that this level could fluctuate with amplitude of 1 m (±0.50 m) around the average value mainly due to hydrodynamics conditions; this interval is indicated on the figure by the shaded zone. This possible range of variation is considered to decrease over the last two millennia.

Tables

Table 1: Chronological episodes distinguished in the late Holocene of the Banc d'Arguin. The intervals between the listed episodes correspond to phases during which no sedimentary structures are registered.

Table 2: Specific data related to the radiocarbon datings used in Figures 3 (Téchekché) and 6 (Iwik), and in table 4. Lab number references : Gd : Gadam Centre, Silesian University of Technology ; Ly: Centre de Datation par le Radiocarbone - UMR5138 - Université Claude Bernard Lyon1 ; Pa: Laboratoire d'Océanographie et du Climat – Paris ; SacA: laboratoire des sciences du climat et de l'environnement (CEA/CNRS/UVSQ); NIA: IRI (Institut des Radio-isotopes – Université Abdou Moumouni – Niamey).

Table 3: Description of the IP properties

Table 4: Altitudes and ages related to the current mean sea level reached by the postglacial transgression during the late Holocene. Except in the case of radiocarbon dates for IP1, IP4 and IP6 (see Table 2), other ages are attributed considering their attachment to a defined paleoshoreline (Table 1).

Table 5: Main trends of various sea level curves in different low-latitude regions of the Earth.

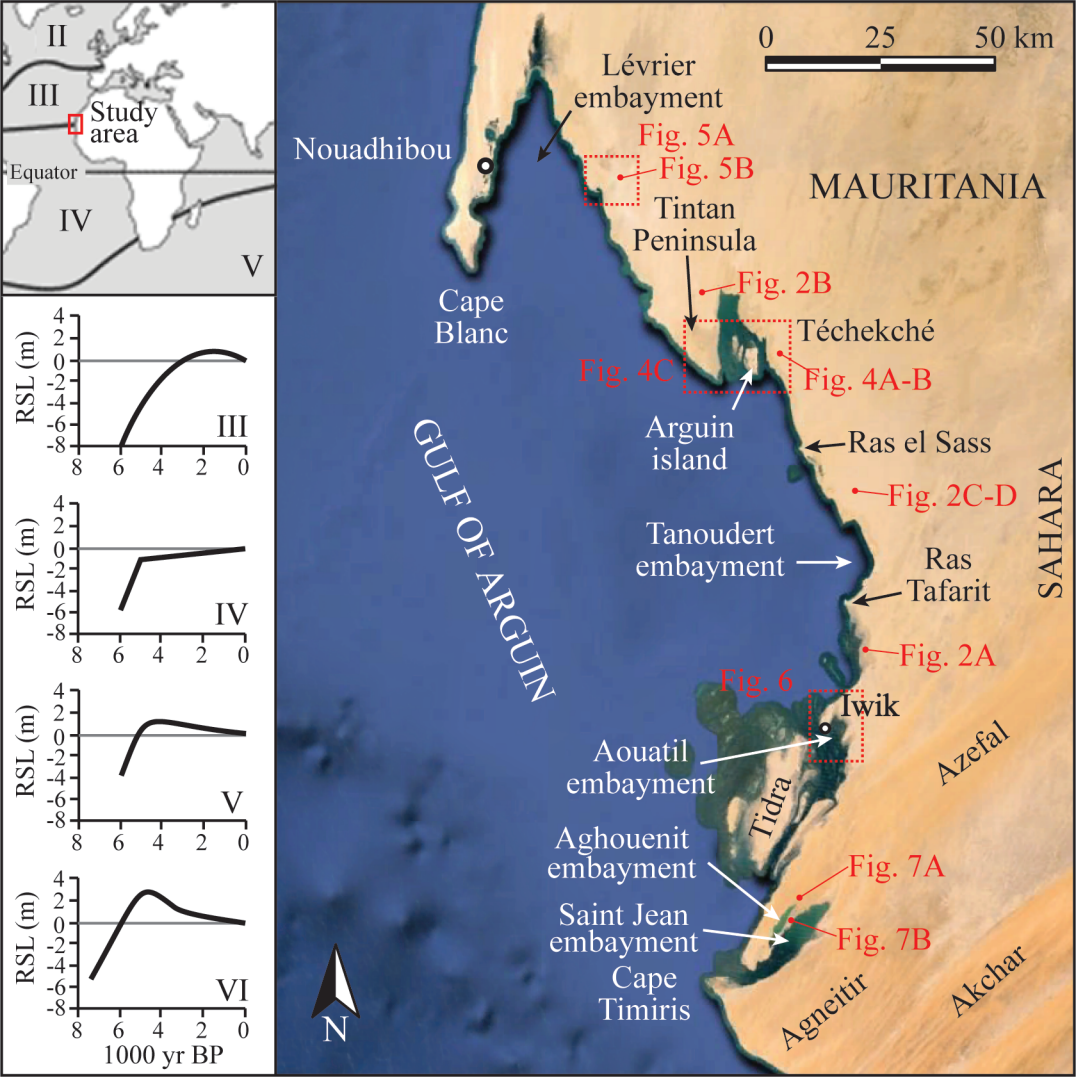
II
III
Study area
Equator
IV
V
RSL (m)
III
IV
V
VI
1000 yr BP
0
25
50 km
Lévrier embayment
Fig. 5A
Fig. 5B
Nouadhibou
MAURITANIA
Tintan Peninsula
Fig. 2B
Cape Blanc
Téchekché
Fig. 4C
Fig. 4A-B
Arguin island
Ras el Sass
GULF OF ARGUIN
Fig. 2C-D
Tanoudert embayment
Ras Tafarit
SAHARA
Fig. 2A
Fig. 6
Iwik
Aouatil embayment
Azefal
Tidra
Aghouenit embayment
Fig. 7A
Saint Jean embayment
Fig. 7B
Cape Timiris
Agneitir
Akchar
N

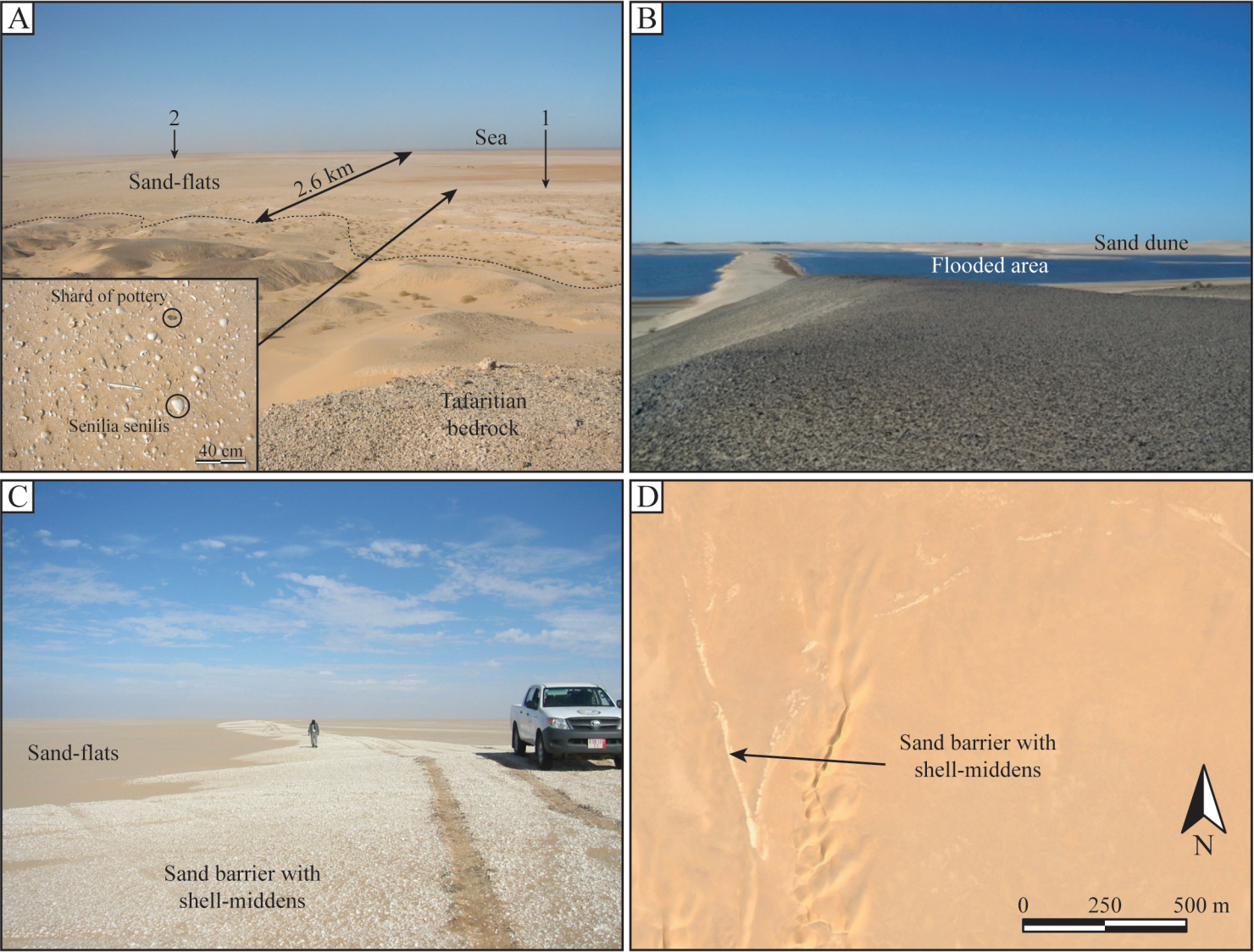
A
2
Sea
1
Sand-flats
2.6 km
Shard of pottery
Senilia senilis
40 cm
Tafaritian
bedrock
B
Sand dune
Flooded area
C
Sand-flats
Sand barrier with
shell-middens
D
Sand barrier with
shell-middens
N
0
250
500 m

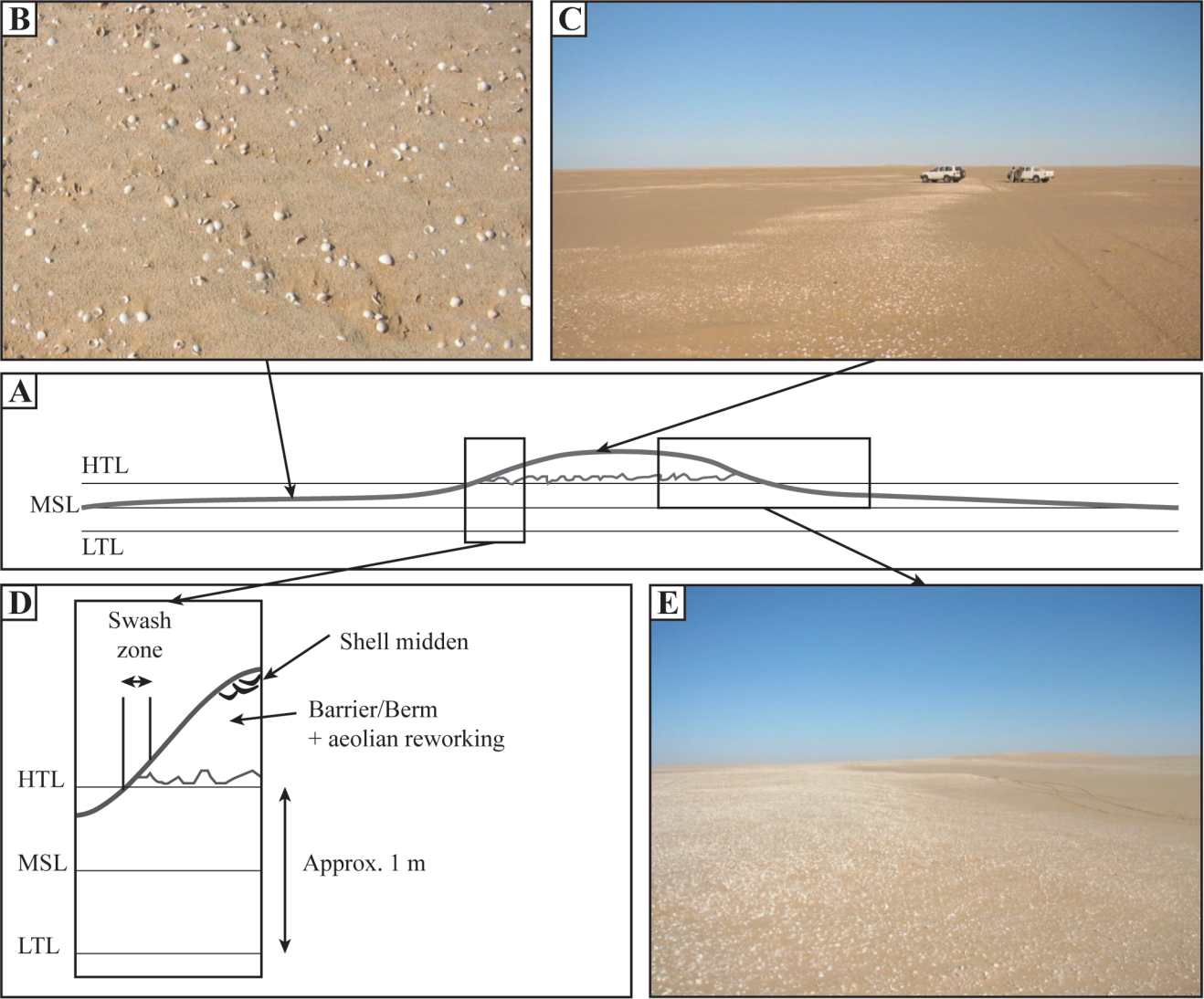
B
C
A
HTL
MSL
LTL
D
Swash
zone
Shell midden
Barrier/Berm
+ aeolian reworking
HTL
MSL
LTL
Approx. 1 m
E

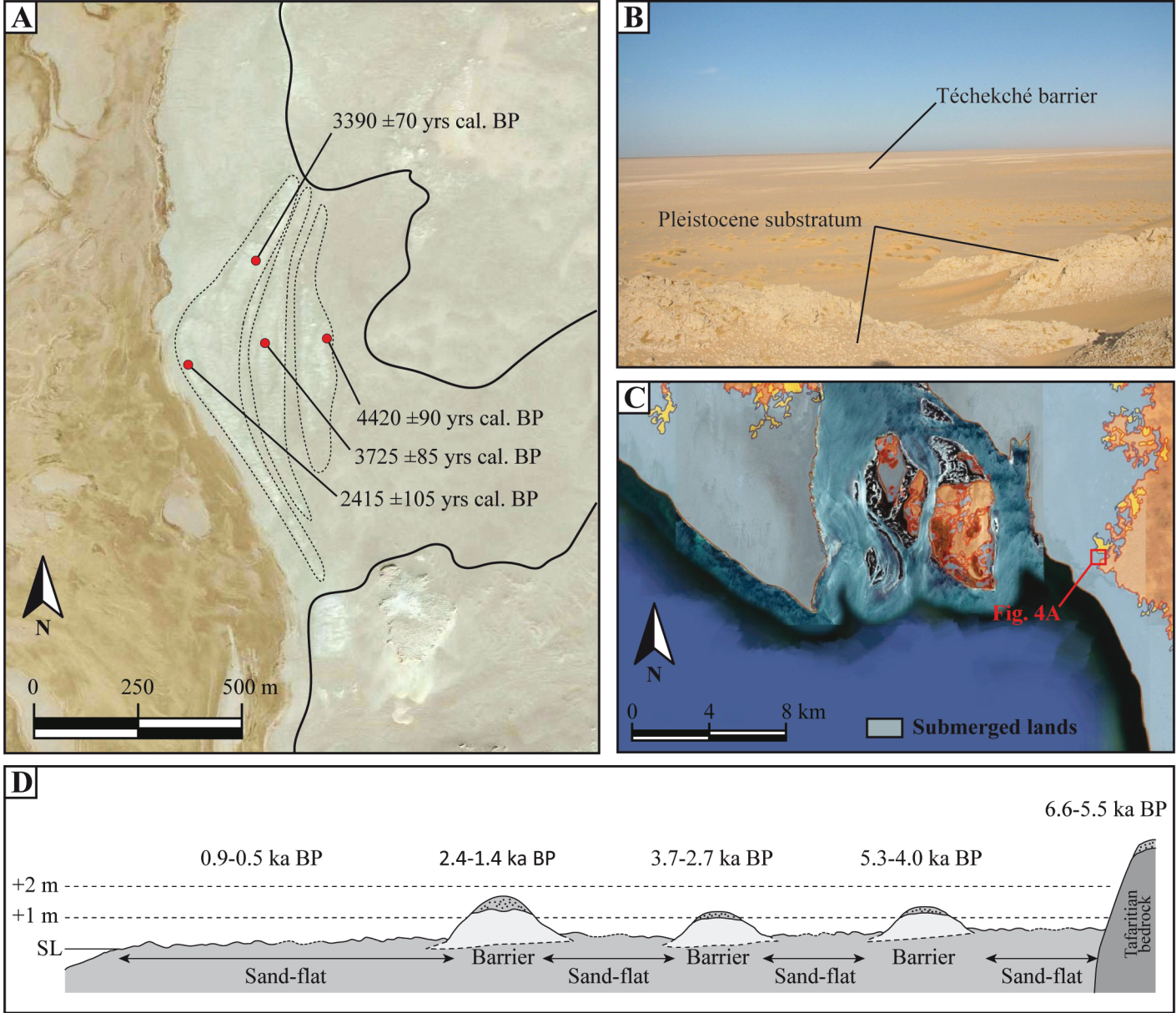
A
3390 ±70 yrs cal. BP
4420 ±90 yrs cal. BP
3725 ±85 yrs cal. BP
2415 ±105 yrs cal. BP
N
0
250
500 m
B
Téchekché barrier
Pleistocene substratum
C
Fig. 4A
N
0
4
8 km
Submerged lands
D
6.6-5.5 ka BP
0.9-0.5 ka BP
2.4-1.4 ka BP
3.7-2.7 ka BP
5.3-4.0 ka BP
+2 m
+1 m
SL
Barrier
Barrier
Barrier
Sand-flat
Sand-flat
Sand-flat
Sand-flat
Tafaritian bedrock

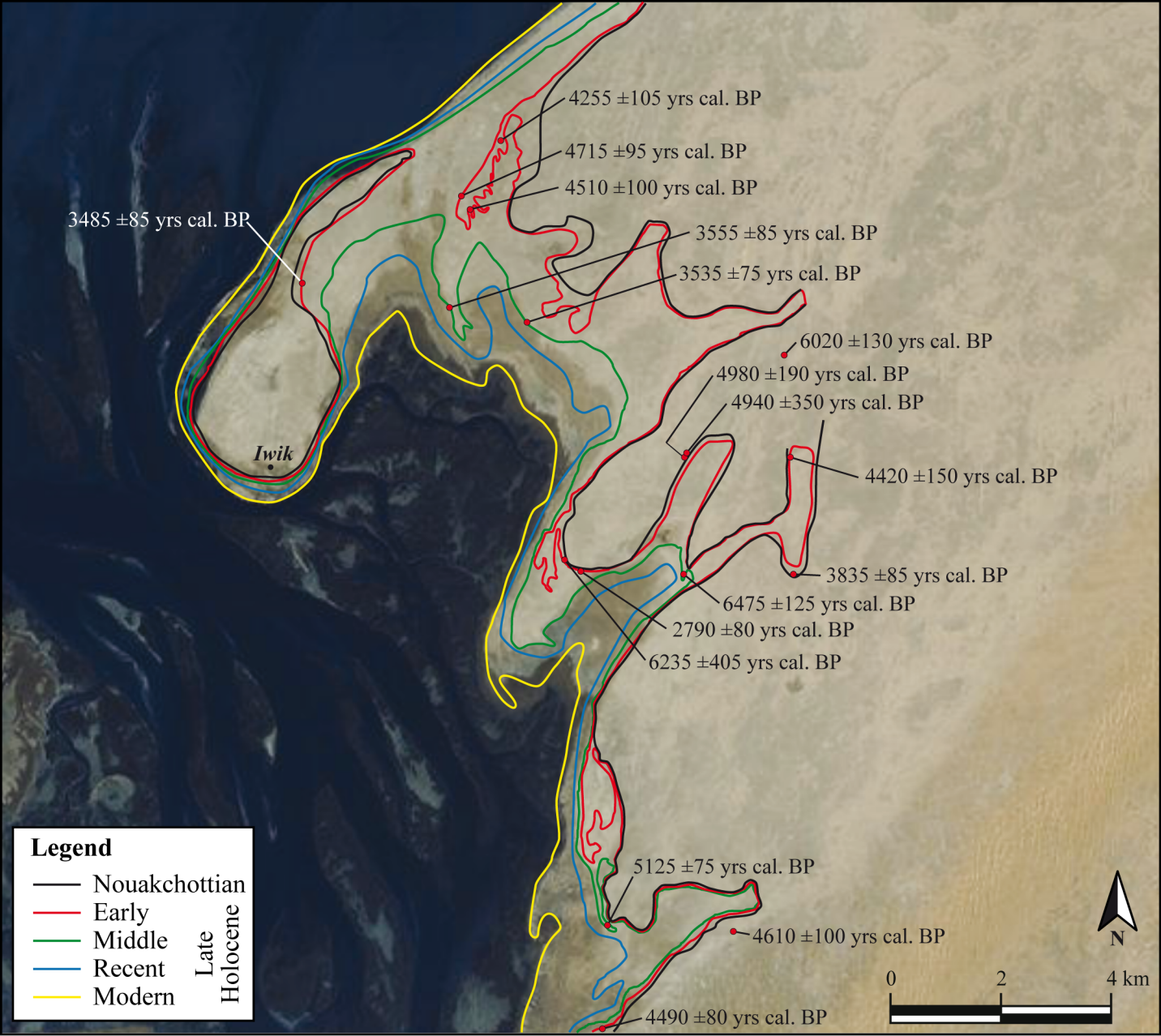
4255 ±105 yrs cal. BP
4715 ±95 yrs cal. BP
4510 ±100 yrs cal. BP
3485 ±85 yrs cal. BP
3555 ±85 yrs cal. BP
3535 ±75 yrs cal. BP
6020 ±130 yrs cal. BP
4980 ±190 yrs cal. BP
4940 ±350 yrs cal. BP
Iwik
4420 ±150 yrs cal. BP
3835 ±85 yrs cal. BP
6475 ±125 yrs cal. BP
2790 ±80 yrs cal. BP
6235 ±405 yrs cal. BP
5125 ±75 yrs cal. BP
4610 ±100 yrs cal. BP
4490 ±80 yrs cal. BP
Legend
Nouakchottian
Early
Middle
Recent
Modern
Late Holocene
N
0
2
4 km

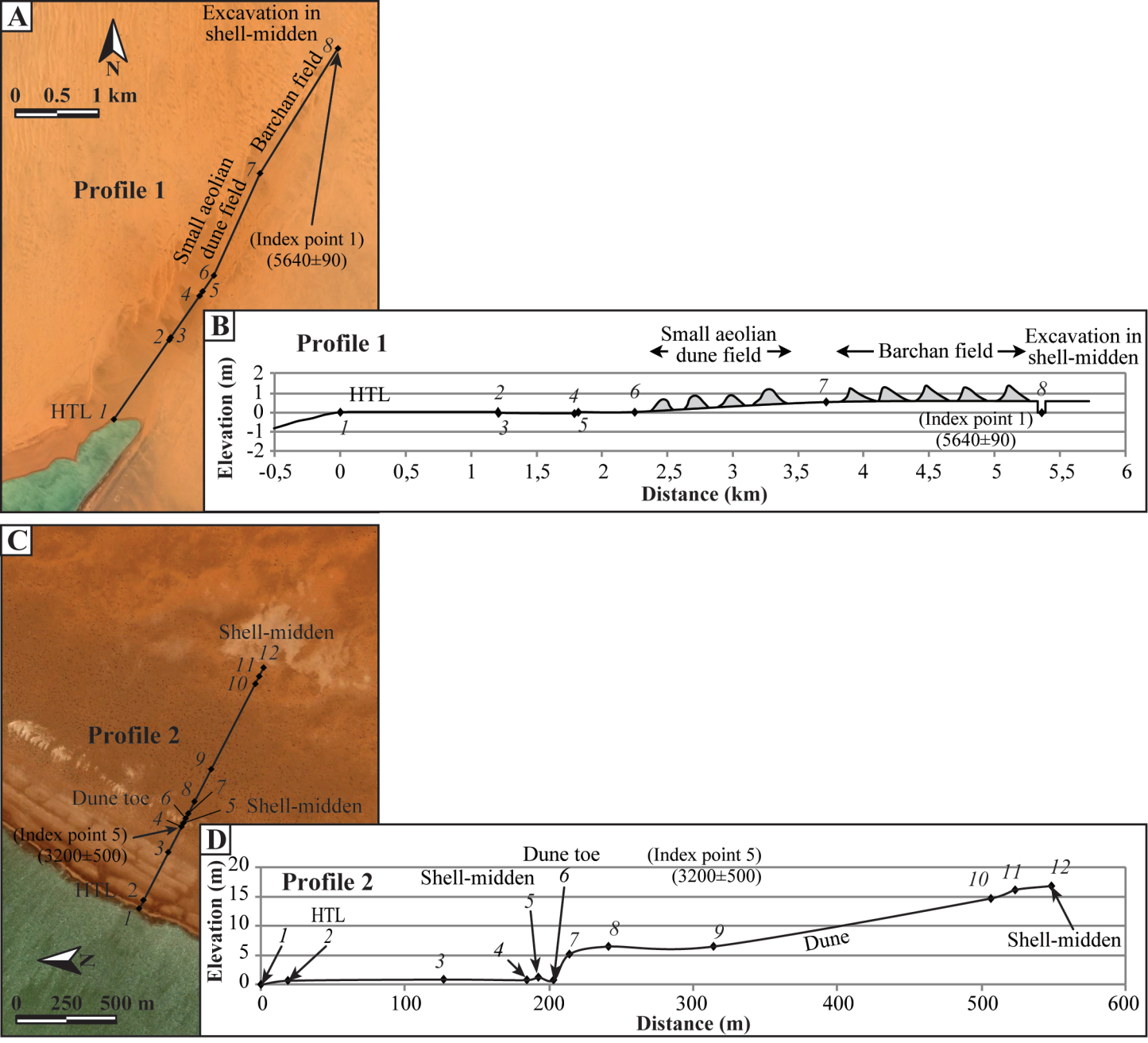
A
Excavation in shell-midden
N
0 0.5 1 km
Barchan field
Small aeolian dune field
Profile 1
(Index point 1)
(5640±90)
HTL 1
B
Profile 1
Small aeolian dune field
Barchan field
Excavation in shell-midden
Elevation (m)
HTL
(Index point 1)
(5640±90)
Distance (km)
C
Shell-midden
Profile 2
Dune toe
Shell-midden
(Index point 5)
(3200±500)
HTL
N
0 250 500 m
D
Profile 2
Dune toe
(Index point 5)
(3200±500)
Shell-midden
HTL
Dune
Shell-midden
Elevation (m)
Distance (m)

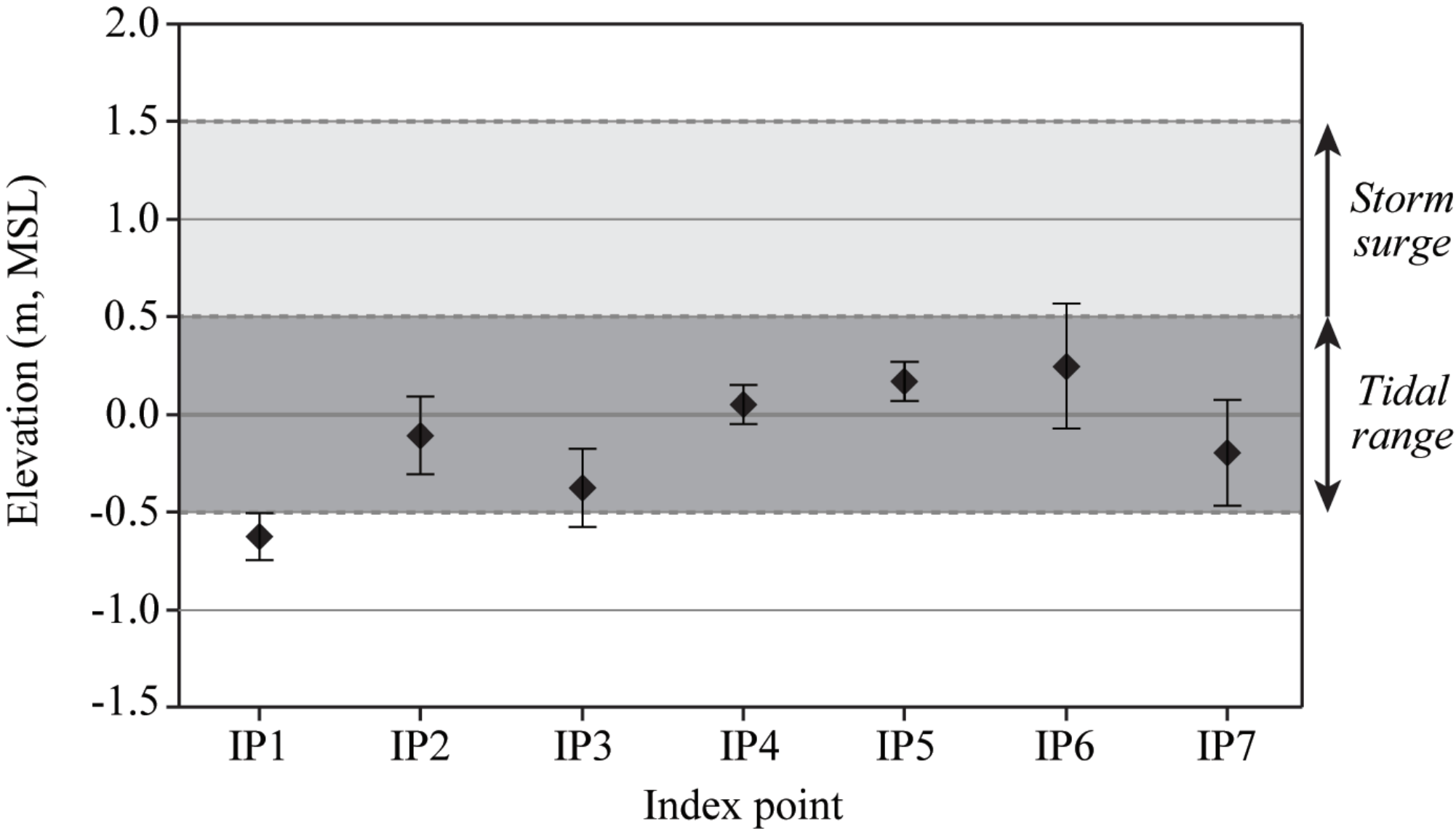
2.0
1.5
1.0
0.5
0.0
-0.5
-1.0
-1.5
Elevation (m, MSL)
IP1
IP2
IP3
IP4
IP5
IP6
IP7
Index point
Storm surge
Tidal range

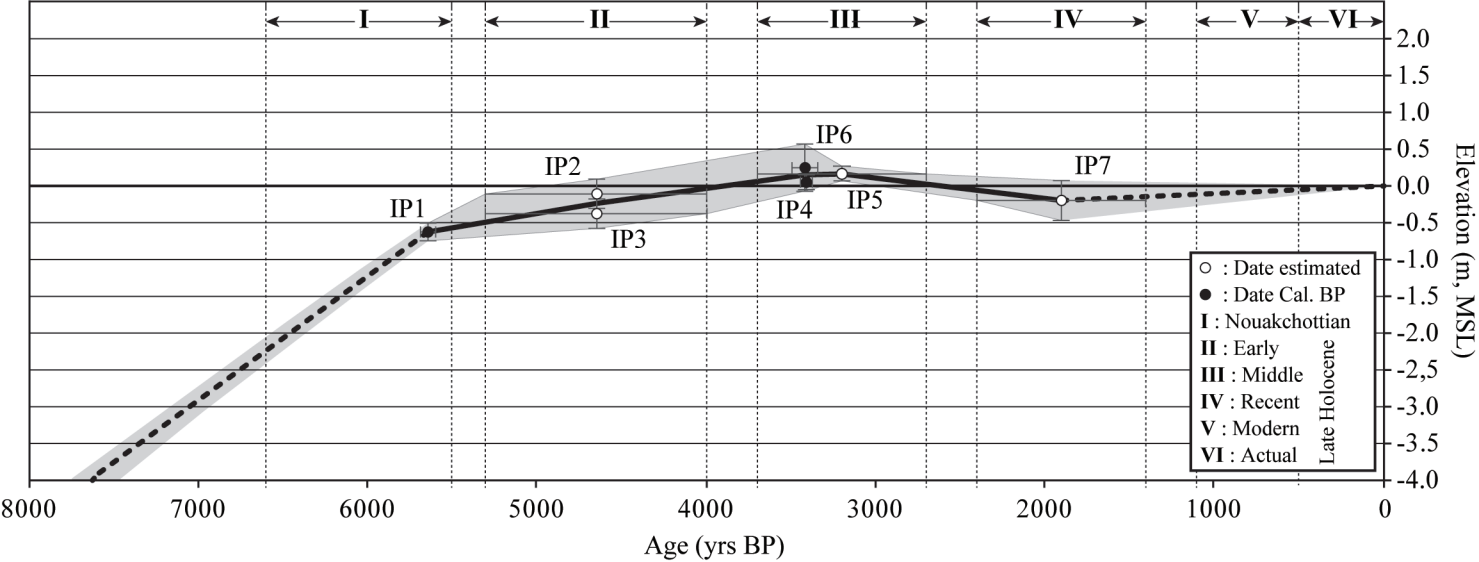
I
II
III
IV
V
VI
IP1
IP2
IP3
IP4
IP5
IP6
IP7
2.0
1.5
1.0
0.5
0.0
-0.5
-1.0
-1.5
-2.0
-2,5
-3.0
-3.5
-4.0
Elevation (m, MSL)
8000
7000
6000
5000
4000
3000
2000
1000
0
Age (yrs BP)
: Date estimated
: Date Cal. BP
I : Nouakchottian
II : Early
III : Middle
IV : Recent
V : Modern
VI : Actual
Late Holocene

Epoch	***Stage***	***Age*** *(kyrs BP)*
Late Holocene	Actual	0.5 - 0.0
	Modern	0.9 - 0.5
	Recent	2.4 - 1.4
	Middle	3.7 - 2.7
	Early	5.3 - 4.0
Nouackchottian		6.6 - 5.5

Point	IP1	IP2	IP3	IP4
Location	Bay of Aghouenit	Bay of Aouatil (Iwik)	Bay of Aouatil (Iwik)	Bay of Aghouenit
Latitude	19°34.47'N	19°53.90'N	19°54.34'N	19°28.20'N
Longitude	16°19.77'W	16°13.87'W	16°14.38'W	16°23.64'W
Episode	Nouakchottian	Early part of late Holocene	Early part of late Holocene	Middle part of late Holocene
Age (yrs BP)	5640 ± 90	4650 ± 650	4650 ± 650	3430 ± 70
Altitude /current HTL (m)	-0,03	+0.64	+0,22	+0,65
Accuracy (m)	±0,05	±0,01	±0,01	±0,01
Berm thickness (m)	0,2	useless	useless	useless
Accuracy (m)	±0,05	/	/	/
Swash height (m)	max. 0,1	max. 0,25	max. 0,25	max. 0,15
Accuracy (m)	±0,1	±0,2	±0,2	±0,1
HTL accuracy (m)	±0,25	±0,25	±0,25	±0,25
MSL (tidal range: 1 m)	-0,63	-0,11	-0,38	0,05
Final accuracy (± ; m)	0,12	0,20	0,20	0,10

IP5	IP6	IP7
Bay of Aghouenit	Bay of Aghouenit	Bay of Aghouenit
19°31.10'N	19°29.16'N	19°30.82'N
16°21.99'W	16°22.97'W	16°21.39'W
Middle part of late Holocene	Middle part of late Holocene	Recent part of late Holocene
3200 ± 500	3450 ± 155	1900 ± 500
+0.77	+0.85	+0.40
±0,01	±0,30	±0,25
useless	useless	useless
/	/	/
max. 0,15	max. 0,15	max. 0,15
±0,1	±0,1	±0,1
±0,25	±0,25	±0,25
0,17	0,25	-0,20
0,10	0,32	0,27

Location	Main results	References
Gulf of Mexico	Morphological manifestations of one or more rising phases and highstands in sea level alternating with falling phases and shoreface adjustment to present sea level. Evidence of sea-level fluctuations of ±1 to 1.5 m from about 5500 to 1200 cal yr BP.	Morton et al 2000
Brazil coast	The RSL shows a highstand elevation about 2.1 m (max. 4 m) lasting between 5000 and 5800 cal yr BP. At the point of maximum transgression, the sea level began a general behavior of lowering until the present.	Angulo et al 2006, Castro et al , 2014
South Africa	RSL rise to 0–3 m above present by 6800 cal yr BP. Sea level was near present between 4.9 and 2.5 ka followed by a drop in sea level of 1–2 m between 2.5 and 1.8 ka. A brief sea-level highstand of approximately 0.5 to 1.0 m at 1.3 cal kyr BP, followed by a lowstand of around –0.5 to –1.0 m at c. 0.7 cal kyr BP.	Compton, 2001 In Horton (2006)
South Australia	A mid Holocene highstand of +1 m (New South Wales and south coast of Western Australia) to +4.5 m (South Australia and Tasmania) between 7500 and 6500 yr, and a	Harvey, 2003 In Horton (2006)

	subsequent fall to present.RSL.	
Vietnam	A mid-Holocene sea-level highstand slightly above +1.4 m was reached between 6.7 and 5.0 ka, with a peak value close to +1.5 m around 6.0 ka. After 5.0 ka sea level dropped and fell almost linearly.	Statteger et al 2013
Indo-pacific zone	The existence of a late Holocene highstand ("3 m beaches" and exposed coral reef terraces) appears to be the general rule in this zone at 6000 cal yr BP	Thom and Roy, 1983 and 1985; Lambeck and Nakada, 1990; Woodroffe and Horton, 2005; Sloss et al., 2007
Hawaï	A new Holocene sea-level curve for Oahu showing mean sea level higher than today between ~5000 and ~2000 yr ago with a maximum ~2 m above present ca. 3500 yr ago. These results correlate with additional evidence from Hawaii and other Pacific islands.	Grossman & Fletcher 2008